Dalton Transactions

RSC Publishing

PAPER

View Article Online
View Journal | View Issue

Cite this: *Dalton Trans.*, 2013, **42**, 10828

Cyclopalladation of dimesityl selenide: synthesis, reactivity, structural characterization, isolation of an intermediate complex with C–H···Pd intra-molecular interaction and computational studies†

Siddhartha Kolay,[a] Amey Wadawale,[a] Dasarathi Das,[a] Hemanta K. Kisan,[b] Raghavan B. Sunoj*[b] and Vimal K. Jain*[a]

Received 9th April 2013,
Accepted 15th May 2013

DOI: 10.1039/c3dt50935d

www.rsc.org/dalton

The reaction of dimesityl selenide (Mes_2Se) with either $PdCl_2(PhCN)_2$ in toluene or $PdCl_2$ in toluene–acetonitrile yields a chloro-bridged binuclear palladium complex, $[Pd_2Cl_2(\mu\text{-}Cl)_2(Mes_2Se)_2]$ (**1**), whereas with Na_2PdCl_4 in refluxing ethanol, a cyclometallated palladium complex, $[Pd_2(\mu\text{-}Cl)_2\{MesSeC_6H_2(Me_2)\text{-}CH_2\}_2]$ (**2**) is afforded. **2** can also be obtained when **1** is refluxed in ethanol. On treatment with $Pb(Epy)_2$ in dichloromethane, **2** afforded the Epy-bridged binuclear complexes, $[Pd_2(\mu\text{-}Epy)_2\{MesSeC_6H_2(Me_2)\text{-}CH_2\}_2]$ (**3**; E = S (**3a**) or Se (**3b**)). Treatment of **2** with PPh_3 yields a bridge-cleaved monomeric complex, $[PdCl\{MesSeC_6H_2(Me_2)CH_2\}(PPh_3)]$. The molecular structures of **1–3** were established by X-ray diffraction analyses. All the complexes are dimeric, with the palladium atoms acquiring a distorted square planar configuration. There are intra-molecular C–H···Pd interactions ($d_{M\text{–}H}$: 2.75 Å and <C–H···Pd: 111.23°) in **1** which facilitate the activation of the C–H (sp^3) bond leading to metallation. The optimized geometry of **1** obtained using the DFT(B3LYP) computational method identified a C–H···Pd contact distance of 2.78 Å. There are two independent molecules of **2** in the unit cell, which differ slightly in bond lengths, bond angles and torsion angles. The mechanism of formation of the dimeric species **2** is examined using DFT (B3LYP) computations.

Introduction

Since the early study of Cope and Siekman,[1] cyclometallated palladium complexes (or palladacycles) have been of considerable interest and have emerged as one of the most important families of organometallic compounds.[2] There are several obvious reasons for this sustained interest in these complexes which can be attributed to their outstanding applications as catalysts (*e.g.*, $[Pd_2(\mu\text{-}OAc)_2\{tol_2PC_6H_4CH_2\text{-}o\}_2]$ by Herrmann and coworkers[3]) in organic synthesis,[3–6] the fact that they are metallomesogenic[7] as well as their intriguing photophysical properties,[8] in materials science[9,10] and their rich reaction chemistry.[2,11]

A plethora of organic compounds containing N, P, As, S donor atoms undergo cyclopalladation (Scheme 1) so as to give, in general, a four-electron C-anionic donor (C^Y) ligand. Although several mechanisms have been proposed for the cyclopalladation reaction, it is generally believed that initially, a ligand is coordinated to the palladium atom and in this intermediate species, the C–H bond is activated only when it is within the metal coordination plane.[4] Such intermediates are seldom isolated, although their existence can be inferred. For instance, the metallation of Me_2ECH_2Ph (E = N, P, As, Sb) shows a pronounced dependence on the size of E. While dimethylbenzylamine and dimethyl benzylphosphine are readily cyclopalladated,[12,13] the dimethylbenzylarsine derivatives, $PdX_2(Me_2AsCH_2Ph)_2$, (X = Cl, Br, I) do not metallate in refluxing 2-ethoxy ethanol both in the presence or absence of a base.[14]

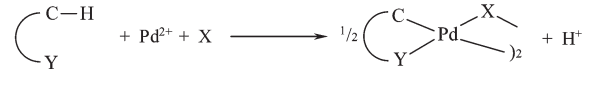

(X = Cl or OAc; Y = N, P, As, S donor atoms; C = ≡C—, =CH—, —CH2-)

Scheme 1

[a]*Chemistry Division, Bhabha Atomic Research Centre, Mumbai 400085, India*
[b]*Department of Chemistry, Indian Institute of Technology Bombay, Powai, Mumbai 400076, India. E-mail: jainvk@barc.gov.in; Fax: +91 22 2550 5151; Tel: +91-22-2559 5095*

†Electronic supplementary information (ESI) available. CCDC 901678–901680 and 930643 for $[Pd_2Cl_2(\mu\text{-}Cl)_2(Mes_2Se)_2]$ (**1**), $[Pd_2(\mu\text{-}Cl)_2\{MesSeC_6H_2(Me_2)CH_2\}_2]$ (**2**), $[Pd_2(\mu\text{-}Spy)_2\{MesSeC_6H_2(Me_2)CH_2\}_2]$ (**3a**) and $[Pd_2(\mu\text{-}Sepy)_2\{MesSeC_6H_2(Me_2)\text{-}CH_2\}_2]$ (**3b**) respectively. For ESI and crystallographic data in CIF or other electronic format see DOI: 10.1039/c3dt50935d

There is extensive literature on cyclopalladated complexes derived from Group 15 donor (N, P, As) ligands. Among the Group 16 donor ligands, only sulfur compounds have been investigated[2,4] and have also been used in C–C coupling reactions as catalysts.[15] Cyclopalladation employing organoselenium ligands is rarely reported, $[Pd_2(\mu\text{-}OAc)_2(C_6H_4SeBu^t)_2]$ being the only complex described so far[16] where palladation takes place through aromatic C–H bond activation. The lack of studies on the cyclometallation of organoselenium ligands could possibly be due to the formation of either simple coordination complexes, $[PdX_2(SeR_2)_2]$ or the cleavage of the Se–C bond under cyclometallation reaction conditions. For example, in an attempt to cyclometallate di-*o*-tolyl selenide with palladium acetate, Singh and coworkers isolated $[Pd(OAc)(Setol\text{-}o)]_4$ formed by the cleavage of the Se–C bond.[17] It is worth noting that palladium complexes with seleno ether ligands show better catalytic activity than the corresponding thio ligands.[18]

With the above perspective, we have examined the reactivity of dimesityl selenide and isolated not only the cyclopalladated complex, but also the intermediate complex with a C–H···Pd intra-molecular interaction. We have also investigated the reactivity of the cyclometallated complex. The results of this work are reported herein.

Experimental section

General

The solvents were dried and distilled under a nitrogen atmosphere prior to use according to a literature method.[19] All the reactions were carried out in a Schlenk flask under a nitrogen atmosphere. Bis(2,4,6-trimethylphenyl)selenide, $(Mes)_2Se$,[20] was prepared according to the reported method and the other reagents were obtained from commercial sources and were used without further purification. Elemental analyses were carried out on a Carlo-Erba EA-1110 CHN-S instrument. Melting points were determined in capillary tubes and are uncorrected. ^{1}H NMR spectra were recorded on a Bruker Avance 500 and Avance II-300 NMR spectrometers operating at 500 and 300 MHz, respectively while ^{77}Se{^{1}H} NMR spectra were recorded on a Bruker Avance II-300 NMR spectrometer operating at 57.24 MHz. The chemical shifts are relative to an internal chloroform peak (δ 7.26 for ^{1}H) and external Me_2Se for ^{77}Se{^{1}H} (secondary reference: Ph_2Se_2 in $CDCl_3$, δ 463 ppm).

X-ray crystallography

Single crystal X-ray data on $[Pd_2Cl_2(\mu\text{-}Cl)_2(Mes_2Se)_2]$ (**1**), $[Pd_2(\mu\text{-}Cl)_2\{MesSeC_6H_2(Me_2)CH_2\}_2]$ (**2**), $[Pd_2(\mu\text{-}Spy)_2\{MesSeC_6H_2(Me_2)CH_2\}_2]$ (**3a**) and $[Pd_2(\mu\text{-}Sepy)_2\{MesSeC_6H_2(Me_2)CH_2\}_2]$ (**3b**) were collected on a SuperNova or Bruker APEX-II CCD diffractometer. The crystallographic data together with the data collection and refinement details are given in Table 1. All the data were corrected for Lorentz and polarization effects. The structures were solved by direct methods[21] and expanded using the Fourier technique.[22] The non-hydrogen atoms were refined anisotropically and fitted with hydrogen atoms in their calculated positions. All the calculations were performed using a crystal structure crystallographic software package.[23,24] The molecular structures were drawn using ORTEP.[25]

Synthesis

$[Pd_2Cl_2(\mu\text{-}Cl)_2(Mes_2Se)_2]$ (1). (i) $PdCl_2(PhCN)_2$ (233 mg, 0.61 mmol) was added to a toluene solution (25 ml) of Mes_2Se (206 mg, 0.65 mmol) and the reaction mixture was stirred at room temperature for 4 h. The solution was dried under vacuum and the residue was washed thoroughly with hexane, diethyl ether and toluene and extracted with dichloromethane, which was evaporated under vacuum to give a brown residue. The latter was recrystallized from dichloromethane containing a few drops of hexane as red crystals (182 mg, 60% yield, m.p.: 193 °C (dec)). Analysis Calcd for $C_{36}H_{44}Cl_4Pd_2Se_2$: C, 43.71; H, 4.48; Found: C, 43.42; H, 4.44%. ^{1}H NMR (500 MHz, $CDCl_3$) δ: 2.22, 2.24, 2.49, 2.65 (s, ratio 4 : 2 : 1 : 6, Me), 6.77, 6.83, 6.85, (s, C_6H_2); ^{77}Se {^{1}H} NMR ($CDCl_3$) δ: 322 ppm.

(ii) $PdCl_2$ (250 mg, 1.41 mmol) was added to a toluene–acetonitrile (5 : 25 cm^{-3}) solution of Mes_2Se (447 mg, 1.41 mmol) and the whole mixture was refluxed at 80 °C for 4 h, whereupon a red precipitate formed which was filtered and washed with hexane, diethyl ether and toluene. The brown solid was extracted with dichloromethane. The solvent was evaporated under reduced pressure to give the title complex (yield: 540 mg, 77%). The NMR data were consistent with the above preparation.

$[Pd_2(\mu\text{-}Cl)_2\{MesSeC_6H_2(Me_2)CH_2\}_2]$ (2). Mes_2Se (480 mg, 1.51 mmol) was added to an ethanolic (25 ml) solution of Na_2PdCl_4 (434 mg, 1.47 mmol) and the reactants were refluxed for 4 h. The solvent was evaporated under reduced pressure and the residue was washed thoroughly with hexane and diethyl ether and then extracted with toluene and dried. The complex was recrystallized from acetone containing a few drops of diethyl ether as rod-like orange crystals (415 mg, 61% yield; m.p.: 165 °C (dec)). Analysis Calcd for $C_{36}H_{42}Cl_2Pd_2Se_2$: C, 47.19; H, 4.62. Found: C, 47.50; H, 4.31%. ^{1}H NMR (500 MHz, $CDCl_3$) δ: 1.91 (s, 4-Me, non-metallated), 2.24, 2.26 (each s, 4- and 6-Me, metallated), 2.40 (br s, 2,6-Me, non-metallated), 3.37 (AB pattern, CH_2, $\Delta\gamma_{AB}$ 46 Hz, J_{AB} = 12.6 Hz), 6.75, 6.78 (each s, C_6H_2 metallated), 6.85 (s, C_6H_2 non-metallated) ppm. ^{77}Se {^{1}H} NMR ($CDCl_3$) δ: 408 ppm.

$[Pd_2(\mu\text{-}Spy)_2\{MesSeC_6H_2(Me_2)CH_2\}_2]$ (3a). $Pb(Spy)_2$ (48 mg, 0.11 mmol) was added to a dichloromethane solution of $[Pd(\mu\text{-}Cl)\{MesSeC_6H_2(Me_2)CH_2\}]_2$ (100 mg, 0.11 mmol) and the contents were stirred overnight at room temperature. The supernatant was passed through Celite and the filtrate was evaporated under reduced pressure to give a red residue. The residue was washed with hexane and diethyl ether and extracted with acetone. The solution was concentrated to 1 cm^{-3} and on the addition of a few drops of diethyl ether gave yellow crystals (98 mg, 84% yield; m.p.: 176 °C). Analysis Calcd for

Table 1 Crystallographic and structural determination data for $[Pd_2Cl_2(\mu\text{-}Cl)_2(Mes_2Se)_2]$ (**1**), $[Pd_2(\mu\text{-}Cl)_2\{MesSeC_6H_2(Me_2)CH_2\}_2]$ (**2**), $[Pd_2(\mu\text{-}Spy)_2\{MesSeC_6H_2(Me_2)CH_2\}_2]$ (**3a**) and $[Pd_2(\mu\text{-}Sepy)_2\{MesSeC_6H_2(Me_2)CH_2\}_2]$ (**3b**)

Complex	$[Pd_2Cl_2(\mu\text{-}Cl)_2(Mes_2Se)_2]$	$[Pd_2(\mu\text{-}Cl)_2\{MesSeC_6H_2(Me_2)CH_2\}_2]$	$[Pd_2(\mu\text{-}Spy)_2\{MesSeC_6H_2(Me_2)CH_2\}_2]$	$[Pd_2(\mu\text{-}Sepy)_2\{MesSeC_6H_2(Me_2)CH_2\}_2]$
Empirical formula	$C_{36}H_{44}Cl_4Pd_2Se_2$	$C_{36}H_{42}Cl_2Pd_2Se_2$	$C_{46}H_{50}N_2Pd_2S_2Se_2$	$C_{46}H_{50}N_2Pd_2Se_4$
Formula weight	989.24	916.32	1065.72	1159.52
Crystal size (mm^3)	0.12 × 0.05 × 0.02	0.03 × 0.03 × 0.01	0.25 × 0.15 × 0.15	0.20 × 0.15 × 0.10
Temperature(K)	100(2)	100(2)	298(2)	298(2)
Diffractometer	SuperNova	SuperNova	Bruker APEX-II CCD	Bruker APEX-II CCD
Radiation	Cu-K_α (1.54184 Å)	Cu-K_α (1.54184 Å)	Mo-K_α (0.71073 Å)	Mo-K_α (0.71073 Å)
Crystal system	Triclinic	Monoclinic	Triclinic	Monoclinic
Space group	$P\bar{1}$	$P2_1/c$	$P\bar{1}$	$C2/C$
a (Å)	8.5654(5)	15.1293(5)	8.735(5)	24.997(5)
b (Å)	11.1973(8)	15.0902(5)	10.919(5)	9.941(5)
c (Å)	11.5045(6)	15.1702(4)	23.272(5)	18.149(5)
α (°)	110.442(6)	90.00	98.092(5)	90.00
β (°)	97.754(5)	97.287(3)	93.574(5)	97.153(5)
γ (°)	109.719(6)	90.00	96.018(5)	90.00
Volume ($Å^3$)	932.46(12)	3435.45(18)	2178.7(17)	4475(3)
ρ_{calcd} (Mg m^{-3})	1.762	1.772	1.625	1.721
Z	1	4	2	4
μ (mm^{-1})/F(000)	12.829/488	12.475/1808	2.626/1064	4.090/2272
θ range (°)	4.2772–66.4884	4.1459–66.4852	2.78–26.48	2.64–26.76
Index range	$-10 \le h \le 10$ $-13 \le k \le 13$ $-13 \le l \le 13$	$-18 \le h \le 17$ $-17 \le k \le 17$ $-18 \le l \le 12$	$-10 \le h \le 10$ $-13 \le k \le 13$ $-27 \le l \le 29$	$-32 \le h \le 33$ $-13 \le k \le 12$ $-24 \le l \le 23$
Reflections collected/unique	13 045/3294	10 027/4265	33 744/8908	5558/3544
Data/restraints/parameters	3294/0/205	5990/0/389	8908/0/498	5558/0/249
Final R_1, ωR_2 indices	0.0291/0.0631	0.0446/0.0895	0.0277/0.0701	0.0336/0.0759
R_1, ωR_2 (all data)	0.0407/0.0676	0.0723/0.1016	0.0393/0.0796	0.0804/0.1013
Goodness of fit on F^2	1.021	0.983	1.111	1.029

$C_{46}H_{50}N_2Pd_2S_2Se_2$: C, 51.84; H, 4.73; N, 2.63; S, 6.02. Found: C, 51.30; H, 4.72; N, 2.02; S, 5.78%. ^{1}H NMR (300 MHz, acetone-d_6) δ: 1.93 (s, 4-Me, non-metallated), 2.22 (s, 4- and 6-Me, metallated), 2.43 (s, 2,6-Me, non-metallated), 3.46 (AX pattern, CH_2, $\Delta\gamma_{AX}$ 135 Hz, J_{AX} = 14 Hz), 6.75 (s, C_6H_2 metallated), 6.88 (s, C_6H_2 non-metallated), 6.10 (t, CH-4, C_5H_4N), 6.81 (t, CH-5, C_5H_4N), 7.13 (d, 7.8 Hz, CH-3, C_5H_4N), 7.74 (d, 5 Hz, CH-6, C_5H_4N) ppm. ^{77}Se {^{1}H} NMR ($CDCl_3$) δ: 406 ppm.

$[Pd_2(\mu\text{-Sepy})_2\{MesSeC_6H_2(Me_2)CH_2\}_2]$ (3b). $Pb(Sepy)_2$ (142 mg, 0.027 mmol) was added to a dichloromethane solution of $[Pd(\mu\text{-Cl})\{MesSeC_6H_2(Me_2)CH_2\}]_2$ (250 mg, 0.027 mmol) and the contents were stirred for 6 h. The solution was dried and the complex was washed with hexane (5 ml × 2). The residue was extracted with toluene and re-crystallized as pale yellow crystals from an acetone–hexane mixture (175 mg, 55% yield; m.p.: 155 °C). Analysis Calcd for $C_{46}H_{50}N_2Pd_2Se_4$: C, 47.65; H, 4.35; N, 2.42. Found: C, 48.37; H, 4.63; N, 2.32 . ^{1}H NMR (300 MHz, $CDCl_3$) δ: 0.80–2.33 (m), 2.69–4.01 (m), 6.12 (d, 7.2 Hz), 6.45 (t, 6.2 Hz), 6.66–6.87 (br, m), 7.38 (d, 4.8 Hz), 7.59 (t, 7.6 Hz), 8.02 (d, 7.8 Hz) ppm. ^{77}Se {^{1}H} NMR ($CDCl_3$) δ: 341, 378, 380, 408.

$[PdCl\{MesSeC_6H_2(Me_2)CH_2\}PPh_3]$. PPh_3 (60 mg, 0.023 mmol) was added to a dichloromethane solution of $[Pd_2(\mu\text{-}Cl_2)\{MesSeC_6H_2(Me_2)CH_2\}_2]$ (102 mg, 0.011 mmol) and the contents were stirred for 10 min. The reaction mixture was dried *in vacuo* and the residue was washed with hexane and extracted with toluene. The toluene extract was dried under vacuum to yield a cream colored solid (114 mg, 71% yield; m.p.: >200 °C). Analysis Calcd for $C_{36}H_{36}ClPdPSe$: C, 60.00; H, 5.04. Found: C, 59.71; H, 5.32%. ^{1}H NMR (300 MHz, $CDCl_3$) δ: 1.95 (s, 4-Me, non-metallated), 2.17, 2.24 (each s, 4- and 6-Me, metallated), 2.69 (br, CH_2), 6.48, 6.70 (each s, 3-,5-H, metallated), 6.88 (s, 3-,5-H, non-metallated), 7.41–7.44 (br, Ph), 7.72–7.78 (br, Ph) ppm. ^{31}P{^{1}H} (300 MHz, $CDCl_3$) δ: 31.7 ppm. ^{77}Se{^{1}H} NMR ($CDCl_3$) δ: 393 (d, ^2J(Se–P) = 167 Hz) ppm.

Computational methods

The reactants, intermediates and transition states were fully optimized in the gas phase at the B3LYP level of theory[26] using the Gaussian09 suite of quantum chemical programs.[27] The hybrid density functional B3LYP is used in conjunction with the LANL2DZ basis set[28] for palladium and the remaining elements were treated with Pople's 6-31G** basis set. All the stationary points were characterized by frequency calculations to authenticate the nature of the transition states (TSs) as having one and only one imaginary frequency representing the desired reaction coordinate. Other minima were characterized by a Hessian index of zero. The Intrinsic Reaction Coordinate (IRC) calculations were performed at the B3LYP level of theory to examine whether the TS on the energy profiles connect to the desired minima.[29] The continuum solvation effects were included through an SMD solvation model.[30] All the stationary points were subjected to single-point energy calculations at the $SMD_{(EtOH)}$/B3LYP/6-31G** level of theory. The Gibbs free energies and enthalpies for all the stationary points in the condensed phase were

obtained by adding the corresponding ZPVE and thermal energies obtained in the gas phase computations to the single point energies.

Results and discussion

The reaction of dimesityl selenide (Mes_2Se) with either $PdCl_2(PhCN)_2$ in toluene or $PdCl_2$ in a toluene–acetonitrile mixture yields a chloro-bridged binuclear palladium complex, $[Pd_2Cl_2(\mu\text{-}Cl)_2(Mes_2Se)_2]$ (**1**) in a fairly good yield. When the reaction with Na_2PdCl_4 in refluxing ethanol was carried out, a cyclometallated palladium complex, $[Pd_2(\mu\text{-}Cl)_2\{MesSeC_6H_2(Me_2)CH_2\}_2]$ (**2**) was isolated (as shown in Scheme 2). In some preparations, **2** in the former and **1** in the latter reactions also formed in very poor yields (<5%) and could be separated conveniently on the basis of their solubility. **2** can also be obtained when **1** was refluxed in ethanol. The density functional theory computations suggest that the formation of **1** and **2** are exoergic, respectively, by −61.2 and −63.3 kcal mol^{-1}. **2**, on treatment with $Pb(Epy)_2$ in dichloromethane, afforded the Epy-bridged binuclear complexes, $[Pd_2(\mu\text{-}Epy)_2\{MesSeC_6H_2(Me_2)CH_2\}_2]$ (**3**; E = S (**3a**) or Se (**3b**)). The thiolato-bridged derivative is exoergic by −84.3 kcal mol^{-1}.[31] Complex **2**, on treatment with PPh_3, results in bridge-cleavage to give a mononuclear product $[PdCl\{MesSeC_6H_2(Me_2)CH_2\}(PPh_3)]$.

The ^1H NMR spectra showed the expected resonances. The spectrum of **2** exhibited resonances attributable to the metallated and non-metallated mesityl group. The metallated CH_2 protons are anisotropic and appear as a distinct AB pattern at a significant downfield of 3.37 ppm with $\Delta\gamma_{AB}$ = 46 Hz, and J_{AB} = 12.6 Hz due to the strong *trans* influence of the metallated carbon. In **3a**, the above mentioned metallated CH_2 showed a distinct AX pattern further downfield at 3.46 ppm with a larger chemical shift difference ($\Delta\gamma_{AX}$ = 135 Hz) and coupling constant (J_{AX} = 14 Hz) in the ^1H NMR spectra. The ^{77}Se NMR spectra of these complexes displayed a single resonance which is deshielded with respect to the free ligand (δ 234 ppm). The ^{77}Se NMR resonances for **2** (408 ppm) and **3a** (406 ppm) are considerably deshielded compared to **1** (322 ppm). Such a large deshielding could be due to the presence of a strong *trans* influencing group (CH_2) *cis* to the selenium in the metallated complexes (**2** and **3a**) rather than the non-metallated derivative (**1**), which has a weak *trans* influencing ligand (Cl). The ^1H NMR spectrum of **3b** was quite complex due to the existence of other isomeric species in solution which were also corroborated by the ^{77}Se NMR spectrum, which displayed resonances attributable to two isomeric forms (*sym-cis* and *sym-trans*). However, only one isomeric form could be crystallized

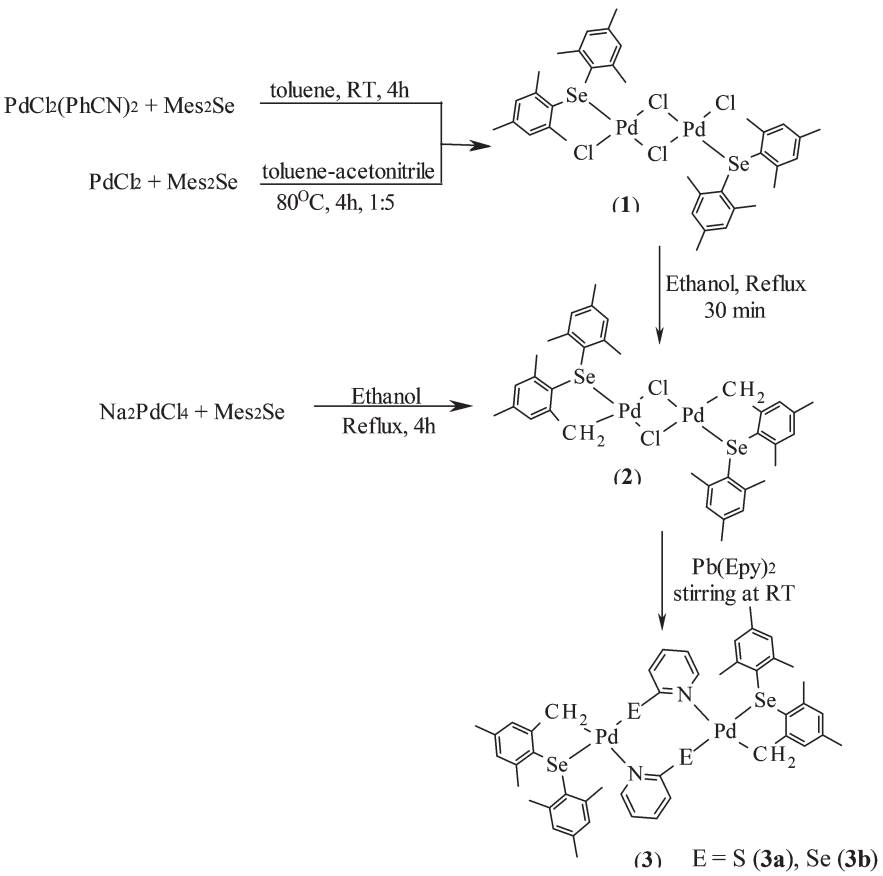

Scheme 2

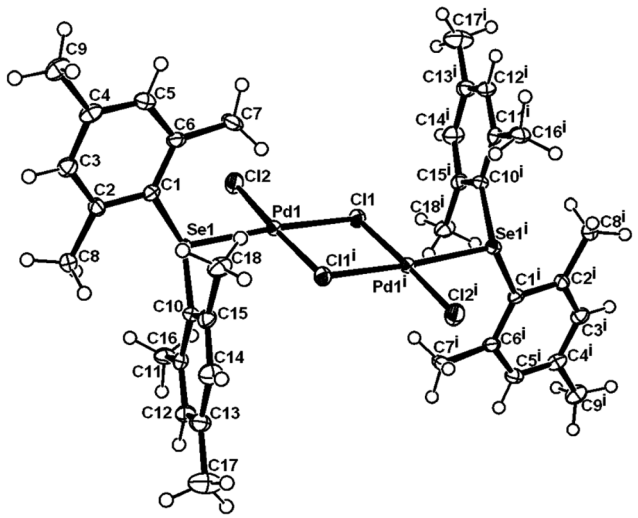

Fig. 1 ORTEP drawing of $[Pd_2Cl_2(\mu\text{-}Cl)_2(Mes_2Se)_2]$ (**1**), the ellipsoids are drawn with 25% probability.

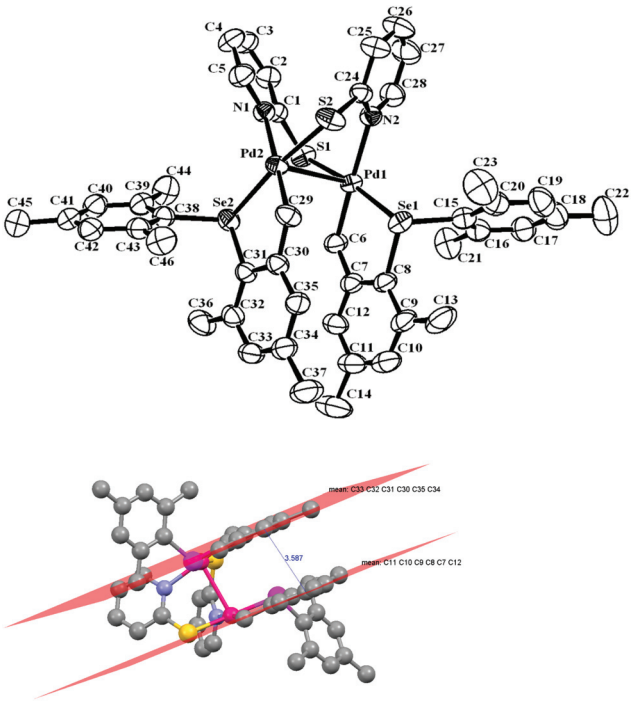

Fig. 3 ORTEP drawing of $[Pd_2(\mu\text{-}Spy)_2\{MesSeC_6H_2(Me_2)CH_2\}_2]$ (**3a**), the ellipsoids are drawn with 25% probability.

from solution. The cyclopalladated complexes, $[Pd_2(Me_2NCH_2C_6H_4)_2\{\mu\text{-}SC_5H_3(R)N\}_2]$ (R = H or Me),[32,33] are known to adopt different isomeric forms and in solution, a dynamic equilibrium may exist between them.[33]

The molecular structures of **1**, **2**, **3a** and **3b**, established by X-ray diffraction analyses, are shown in Fig. 1–4. Selected interatomic parameters are summarized in Tables 2–5. All the complexes are dimeric, with the palladium atoms acquiring a distorted square planar configuration. The Pd–Se distances are well within the range reported in palladium selenolate complexes, such as $[PdCl(SeCH_2CH_2NMe_2)]_3$,[34] $[Pd(OAc)(SeCH_2CH_2CH_2NMe_2)]_2$[35] and $[Pd(OAc)(SeC_6H_4Me\text{-}2)]_4$.[17]

Complex **1**, a centrosymmetric dimer, comprises a chloro-bridged "$Pd_2(\mu\text{-}Cl)_2$" core. The coordinated seleno ether ligands are mutually *trans*. The Pd–$Cl_{(bridging)}$ distances are longer than the terminal Pd–Cl distance. The Pd–$Cl_{bridging}$ *trans* to the seleno ether ligand is marginally longer than the one *trans* to the terminal chloride ligand. The C1–Se1–C10 angle is 104.08°. The mesityl ring lies ~7° above the Pd_2Cl_2 plane so as to result in a intra-molecular C–H···Pd interaction. The Pd···H7C distance and Pd···H7C–C7 angle are 2.75 Å and 111.23° respectively. The bond distance and angle indicate that this interaction is agostic in nature. The Pd···H7C and Cl2···H7B distances are smaller than the sum of their van der Waals radii, 2.75 *vs.* 2.83 Å and 2.86 *vs.* 2.95 Å, respectively. These interactions support the involvement of the metal center in C–H (sp^3) bond activation leading to metallation. The above proposed mechanism of agostic interaction-driven

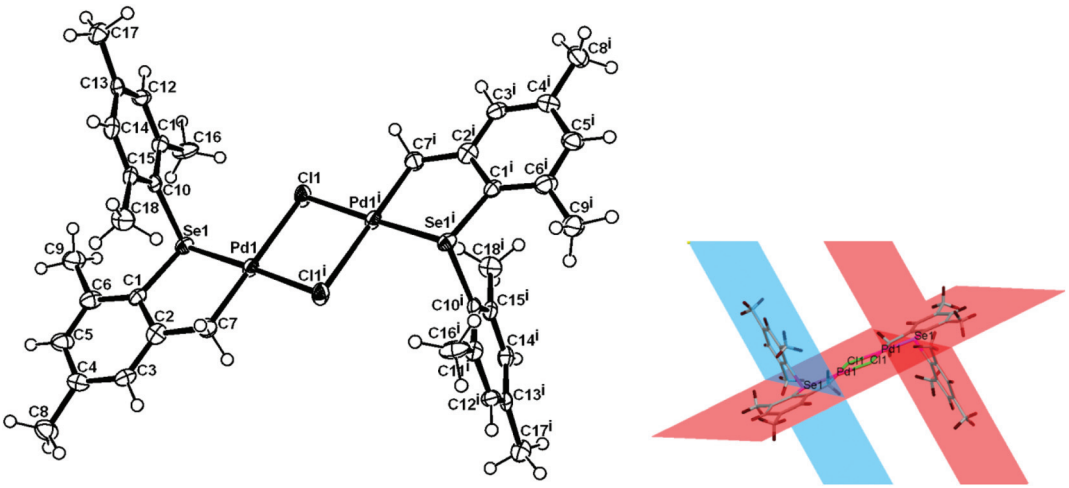

Fig. 2 ORTEP drawing of $[Pd_2(\mu\text{-}Cl)_2\{MesSeC_6H_2(Me_2)CH_2\}_2]$ (**2**) and relative orientation of the rings, the ellipsoids are drawn with 50% probability.

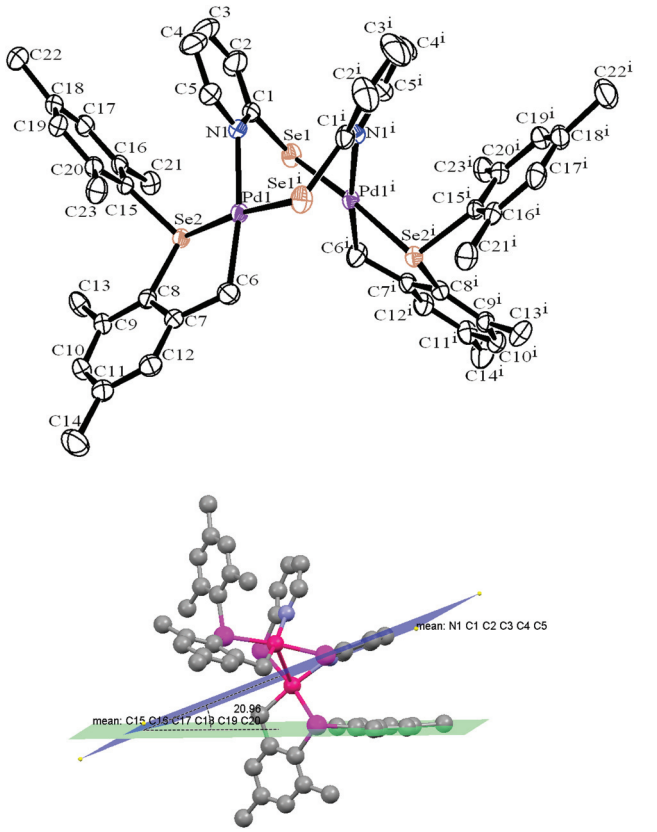

Fig. 4 ORTEP drawing of $[Pd_2(\mu\text{-Sepy})_2\{MesSeC_6H_2(Me_2)CH_2\}_2]$ (**3b**); ellipsoids are drawn with 25% probability.

benzylic C–H bond activation is also supported by theoretical calculations, as discussed letter. The optimized structural parameters, as obtained through the DFT(B3LYP) computations, are in good general agreement with the experimental (X-ray) values.

There are two independent half molecules of **2** in the unit cell, which differ slightly in bond lengths, bond angles and torsion angles. Only one of these is shown in Fig. 2. The molecule adopts a *sym-trans* configuration. In contrast to molecule **1**, where both the mesityl rings of the seleno ether are nearly perpendicular to the central Pd_2Cl_2 plane, in molecule **2**, one of the mesityl ring comes into the central Pd_2Cl_2 plane to satisfy the square planar geometry around palladium, while the non-metallated mesityl rings remain nearly perpendicular (86.17° for molecule **a** and 83.86° for molecule **b**) to the planar metallated PdCCCSe rings. The two five-membered planar metallated PdCCCSe rings are co-planar with the four-membered rectangular Pd_2Cl_2 ring. The coordination around each palladium atom is defined by two Cl atoms and a C and Se atom of the metallated seleno ether. The two bridging Pd–Cl distances are distinctly different. The one *trans* to the metallated carbon atom is longer than the one *trans* to the selenium, owing to the strong *trans* influence of the CH_2 group. This is in good agreement with the reported values (*e.g.* $[Pd_2(\mu\text{-}Cl)_2(py\text{-}C_6H_4)_2]$; Pd–Cl = 2.426(1), 2.349(2) Å.[36] The Pd–C [8,36] and Pd–Se[18] distances conform with the reported values (*e.g.*, $[PdCl\{OC_6H_4C(Ph) = NCH_2CH_2SePh\}]$, Pd–Se = 2.3575(6) Å).[18] The Pd···Pd separation of ~3.45 Å is within the range observed in chloro-bridged cyclometallated palladium complexes (~3.5 Å).[2]

Table 3 Selected bond lengths (Å) and angles (°) of $[Pd_2(\mu\text{-}Cl)_2\{MesSeC_6H_2(Me_2)CH_2\}_2]$ (**2**). The theoretical values are obtained at the B3LYP/6-31G**, LANL2DZ(Pd) level of theory

	Molecule a			
	Experimental	Theoretical	Molecule b	
Pd1–Se1	2.3438(8)	2.423	Pd2–Se2	2.3342(9)
Pd1–C7	2.024(7)	2.042	Pd2–C25	2.039(7)
Pd1–Cl1	2.4786(17)	2.564	Pd2–Cl2	2.4833(17)
Pd1–Cl1^i	2.3739(16)	2.445	Pd2–Cl2^i	2.3713(17)
Se1–C1	1.912(7)	1.938	Se2–C19	1.925(7)
Se1–C10	1.948(6)	1.955	Se2–C28	1.946(7)
Pd1–Pd1^i	3.472	3.559	Pd2–Pd2^i	3.440
Se1–Pd1–Cl1	93.02(4)	95.18	Se2–Pd2–Cl2	92.72(5)
Se1–Pd1–Cl1^i	177.92(5)	174.91	Se2–Pd2–Cl2^i	176.84(5)
Se1–Pd1–C7	87.22(19)	86.49	Se2–Pd2–C25	87.0(2)
C7–Pd1–Cl1	179.7(2)	178.08	C25–Pd2–Cl2	179.3(2)
C7–Pd1–Cl1^i	91.1(2)	89.85	C25–Pd2–Cl2^i	90.5(2)
Cl1–Pd1–Cl1^i	88.67(6)	88.53	Cl2–Pd2–Cl2^i	89.78(6)
Pd1–C7–C2	117.0(5)	118.17	Pd2–C25–C20	117.4(5)
Pd1–Se1–C1	98.5(2)	97.37	Pd2–Se2–C19	98.6(2)
Pd1–Se1–C10	107.49(19)	110.52	Pd2–Se2–C28	107.62(19)
Pd1–Cl1–Pd1^i	91.33(6)	90.52	Pd2–Cl2–Pd2^i	90.22(6)

Table 2 Selected bond lengths (Å) and angles (°) of $[Pd_2Cl_2(\mu\text{-}Cl)_2(Mes_2Se)_2]$ (**1**). The theoretical values are obtained at the B3LYP/6-31G**, LANL2DZ(Pd) level of theory

	Experimental	Theoretical		Experimental	Theoretical
Se1–Pd1	2.3837(5)	2.464	Pd1–Cl1	2.3504(9)	2.439
Pd1–Cl1^i	2.3307(10)	2.444	C1–Se1	1.947(4)	1.951
Pd1–Cl2	2.2810(10)	2.328	C10–Se1	1.945(4)	1.958
			Pd···Pd	3.452	3.551
Cl1–Pd1–Se1	172.57(3)	172.71	Cl2–Pd1–Cl1^i	176.37(3)	177.29
Cl1^i–Pd1–Se1	97.51(3)	88.23	C1–Se1–Pd1	116.04(11)	112.84
Cl2–Pd1–Se1	86.04(3)	94.32	C10–Se1–Pd1	103.38(11)	114.44
Cl1^i–Pd1–Cl1	84.96(3)	86.08	C10–Se1–C1	104.08(16)	104.84
Cl2–Pd1–Cl1	91.42(3)	91.28	Pd1–Cl1–Pd1^i	95.04(3)	93.37

Table 4 Selected bond lengths (Å) and angles (°) of $[Pd_2(\mu\text{-Spy})_2\{MesSeC_6H_2(Me_2)CH_2\}_2]$ (**3a**). The theoretical values are obtained at the B3LYP/6-31G**, LANL2DZ-(Pd) level of theory

	Experimental	Theoretical		Experimental	Theoretical
Pd1–Se1	2.4005(12)	2.477	Pd2–Se2	2.4184(6)	2.476
Pd1–C6	2.037(3)	2.061	Pd2–C29	2.025(3)	2.062
Pd1–S1	2.3136(13)	2.399	Pd2–S2	2.3218(9)	2.398
Pd1–N2	2.179(2)	2.242	Pd2–N1	2.171(2)	2.242
Se1–C8	1.924(3)	1.937	Se2–C31	1.919(3)	1.936
Se1–C15	1.950(3)	1.955	Se2–C38	1.949(3)	1.955
			Pd1–Pd2	2.9288(9)	3.033
Se1–Pd1–S1	172.71(2)	172.19	Se2–Pd2–S2	172.12(2)	172.19
Se1–Pd1–C6	85.94(8)	85.66	Se2–Pd2–C29	85.05(8)	85.66
Se1–Pd1–N2	96.86(6)	94.94	Se2–Pd2–N1	96.85(6)	94.95
C6–Pd1–N2	174.19(11)	173.15	C29–Pd2–N1	176.47(10)	173.13
C6–Pd1–S1	86.89(9)	86.53	C29–Pd2–S2	87.70(8)	86.53
S1–Pd1–N2	90.40(6)	92.82	S2–Pd2–N1	90.55(7)	92.82
Pd1–Se1–C8	97.89(10)	96.94	Pd2–Se2–C31	97.09(9)	96.92
Pd1–Se1–C15	114.57(8)	110.92	Pd2–Se2–C38	118.57(8)	110.97
C8–Se1–C15	102.35(12)	105.49	C31–Se2–C38	103.39(12)	105.47
S1–Pd1–Pd2–S2	−122.78(3)	−126.80	Se1–Pd1–Pd2–S2	64.56(3)	60.84
S1–Pd1–Pd2–Se2	64.91(2)	60.85	Se1–Pd1–Pd2–Se2	−107.749(19)	−111.49

Table 5 Selected bond lengths (Å) and angles (°) of $[Pd_2(\mu\text{-Sepy})_2\{MesSeC_6H_2(Me_2)CH_2\}_2]$ (**3b**). The theoretical values are obtained at the B3LYP/6-31G**, LANL2DZ(Pd) level of theory

	Experimental	Theoretical		Experimental	Theoretical
C6–Pd1	2.045(4)	2.068	C1–Se1	1.900(5)	1.904
N1–Pd1	2.154(3)	2.241	$Pd1^i$–Se1	2.4197(8)	2.496
$Pd1^i$–Pd1	3.1429(8)	3.078	C15–Se2	1.953(4)	1.954
$Se1^i$–Pd1	2.4197(8)	2.491	C8–Se2	1.934(4)	1.942
Se2–Pd1	2.4156(8)	2.507			
C6–Pd1–N1	171.26(16)	176.05	C15–Se2–Pd1	106.71(11)	108.01
C6–Pd1–$Pd1^i$	110.18(14)	101.26	C8–Se2–Pd1	95.84(12)	95.26
C6–Pd1–$Se1^i$	87.92(12)	87.78	C1–N1–Pd1	124.9(3)	125.85
C6–Pd1–Se2	84.15(13)	83.43	C5–N1–Pd1	115.4(3)	114.72
$Se1^i$–Pd1–$Pd1^i$	78.396(16)	81.56	N1–Pd1–$Pd1^i$	78.53(9)	88.98
Se2–Pd1–$Pd1^i$	104.033(16)	101.42	N1–Pd1–$Se1^i$	94.77(9)	92.73
Se2–Pd1–$Se1^i$	172.059(19)	171.11	N1–Pd1–Se2	93.13(9)	95.93
C1–Se1–$Pd1^i$	102.04(13)	103.29			
Se1–$Pd1^i$–Pd1–$Se1^i$	−142.25	−130.96	$Se1^i$–Pd1P–$d1^i$–$Se2^i$	45.50	56.96
Se2–Pd1–$Pd1^i$–$Se2^i$	−126.74	−114.54	Se1–$Pd1^i$–Pd1–Se2	45.50	57.52

The two palladium atoms in **3a** and **3b** are held together by bridging pyridyl chalcogenolate groups (Epy), forming an eight-membered ring which adopts a distorted twist boat conformation. The chalcogen atoms of the Epy ligands are *trans* to the Se atoms of the metallated ligand resulting in an *anti* configuration, which is generally observed for $Pd_2(\mu\text{-Spy})_2L_4$ type complexes.[8,37,38] The configuration around the palladium in both the complexes is distorted square planar but the mutual orientation of the square planes are different for **3a** and **3b**. The angle between the square planes S1Pd1Se1N2 and S2Pd2Se2N1 is 20.97° in **3a** and between Se1Pd1^{i}N1^{i}Se2^i and Se2Pd1Se1^{i}N1 is 39.02° in **3b**, resulting in different orientations of the metallated mesityl ring in the two complexes. The metallated mesityl rings of **3a** display fairly good intramolecular π–π stacking with an angle of 2.04° between the planes and average stacking separation of 3.587 Å. This type of interaction is absent in **3b**. The Pd–S, Pd–N and Pd–C distances are in accord with those reported in $[Pd_2(\mu\text{-Spy})_2(Me_2NCH_2C_6H_4\text{-}C,N)_2]$,[32] $[Pd_3(\mu\text{-Spy})_2(Me_2NCH_2C_6H_4\text{-}C,N)_3][BF_4]$[33] and $[Pd_2(\mu\text{-SCNCH}_2CH_2NMe)_2(Bzq)_2]$.[8] The Pd–Se distances can be compared with $[Pd_2(\mu\text{-SePh})_2(C_{10}H_6NMe_2\text{-}C,N)_2]$[11] and $[Pd_2(\mu\text{-SePh})_2(Me_2NCH_2C_6H_4\text{-}C,N)_2]$.[32] The Pd···Pd distance in **3a** (2.9288(9) Å) is within the generally acceptable range of intra-molecular Pd···Pd interactions (<3.00 Å), while in the corresponding selenolate complex (**3b**) it is much longer (3.143 Å). In complex **3a**, one of the mesityl rings on both the selenium ligands are parallel to each other and are separated by 3.587 Å, which may be attributed to π-stacking, and are positioned on the opposite side of the pyridine thiolate rings. In **3b**, one mesityl group on each of the $Se(Mes)_2$ ligands is also almost but not exactly parallel to the Sepy rings.

Density functional theory computations have been carried out to gain additional insight on the mechanism for the

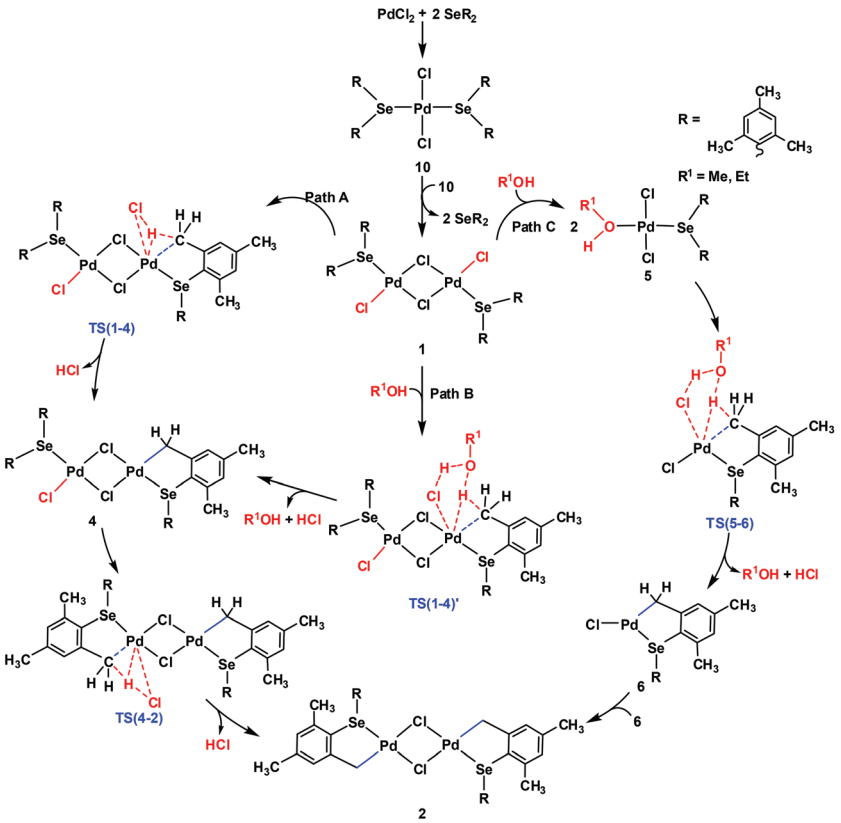

Scheme 3 Mechanistic pathways for the formation of **2** $[Pd_2(\mu\text{-}Cl)_2\{MesSeC_6H_2(Me_2)CH_2\}_2]$ through aryl C–H bond activation.

formation of compound **2**. While several pathways could be envisaged as likely under the experimental conditions, we have presented those which are computed to exhibit lower energies. All the higher energy possibilities are described in the ESI (Fig. S5–S8, Schemes S1–S4†). The most likely mechanistic scenarios are summarized in Scheme 3 and the computed energies are provided in Fig. 5. The first key step involves the conversion of *trans*-$[PdCl_2(Mes_2Se)_2]$ (**10**) to the chloro-bridged dimer **1**. One of the methyl C–H bonds that remains closest to the palladium is activated in such a way that it combines with the chloride ligand to form HCl. The expulsion of HCl would furnish a monocyclopalladated intermediate **4**. The transition states for the formation of HCl from both palladium atoms are located. These transition states **TS(1–4)** and **TS(4–2)**, as shown in Fig. 6, are of very similar energies. It can further be noticed from the computed energy profile that the C–H activation with

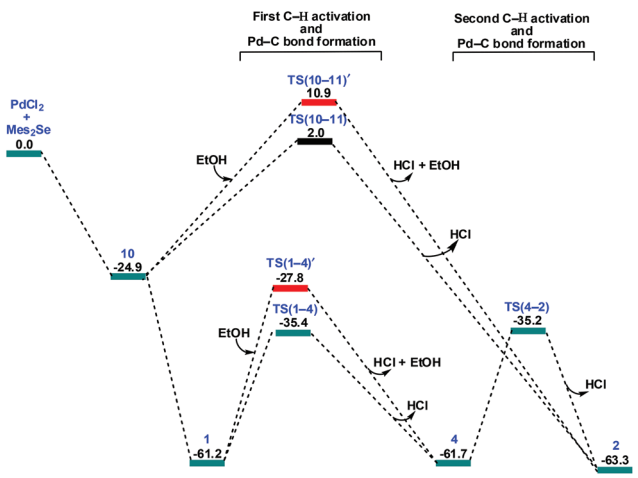

Fig. 5 Gibbs free energy profile (in kcal mol^{-1}) for the formation of $[Pd_2(\mu\text{-}Cl)_2\{MesSeC_6H_2(Me_2)CH_2\}_2]$ (**2**) from $PdCl_2$ and Mes_2Se obtained at the $SMD_{(EtOH)}$/B3LYP/6-31G**//B3LYP/6-31G** level of theory.

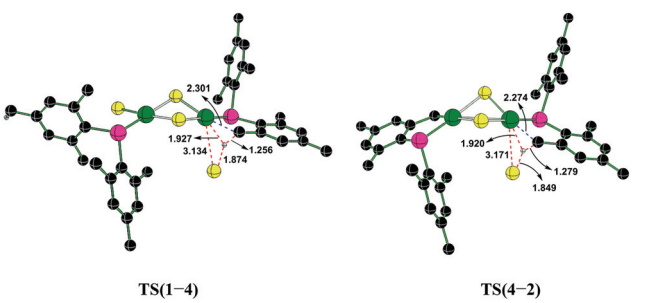

Fig. 6 Optimized geometries of the important transition states (B3LYP/6-31G**, LANL2DZ(Pd) level of theory) involved in the formation of palladacycles **4** and **2**. Distances are in Å. Only select hydrogen atoms are shown. Atom colors: C, black; H, ivory; O, red; Cl, yellow; Pd, green; Se, pink.

the assistance of methanol, designated as pathways B and C, is of higher energy than the unassisted process.

Conclusion

Cyclopalladation of an organoselenium ligand, dimesityl selenide, is accomplished in mild reaction conditions. The possible intra-molecularly coordinated Pd···HC intermediate is isolated. The cyclopalladated complex serves as a useful precursor for the synthesis of other derivative containing metallated selenium ligands. The computed energy profile shows that the methanol assisted C–H activation is of higher energy than the unassisted process.

Acknowledgements

We thank Dr S. K. Sarkar for his encouragement of this work and Prof. U. P. Singh, IIT Roorkee for his help in recording some of the single crystal XRD data. IIT Bombay computer center is acknowledged for the computing time.

References

1 A. C. Cope and R. W. Siekman, *J. Am. Chem. Soc.*, 1965, **87**, 3272.
2 V. K. Jain and L. Jain, *Coord. Chem. Rev.*, 2005, **249**, 3075.
3 M. Beller, H. Fischer, W. A. Herrmann, K. Öfele and C. Brossmer, *Angew. Chem., Int. Ed. Engl.*, 1995, **34**, 1848.
4 J. Dupont, C. S. Consorti and J. Spencer, *Chem. Rev.*, 2005, **105**, 2527.
5 I. Omae, *J. Organomet. Chem.*, 2007, **692**, 2608.
6 M. Albrecht, *Chem. Rev.*, 2010, **110**, 576.
7 P. Espinet, M. A. Esteruelas, L. A. Oro, J. L. Serrano and E. Sola, *Coord. Chem. Rev.*, 1992, **117**, 215.
8 M. D. Santana, R. Garcia-Bueno, G. Garcia, G. Sanchez, J. Garcia, J. Perez, L. Garcia and J. L. Serrano, *Dalton Trans.*, 2011, **40**, 3537.
9 M. Ghedini, I. Aiello, A. Crispini, A. Golemme, M. La Deda and D. Pucci, *Coord. Chem. Rev.*, 2006, **250**, 1373.
10 D. A. Alonso and C. Najera, *Chem. Soc. Rev.*, 2010, **39**, 2891.
11 N. D. Ghawale, S. Dey, V. K. Jain and M. Nethaji, *Inorg. Chim. Acta*, 2008, **361**, 2462.
12 M. Pfeffer, *Inorg. Synth.*, 1989, **26**, 211.
13 H. P. Abicht and K. Z. Issleib, *Z. Anorg. Allg. Chem.*, 1983, **500**, 31.
14 P. P. Phadnis, V. K. Jain, A. Klein, M. Weber and W. Kaim, *Inorg. Chim. Acta*, 2003, **346**, 119.
15 D. Zim, A. S. Gruber, G. Ebeling, J. Dupont and A. L. Monteiro, *Org. Lett.*, 2000, **2**, 2881.
16 Q. Yao, E. P. Kinney and C. Zheng, *Org. Lett.*, 2004, **6**, 2997.
17 T. Chakraborty, S. Sharma, H. B. Singh and R. J. Butcher, *Organometallics*, 2011, **30**, 2525.
18 A. Kumar, M. Agarwal, A. K. Singh and R. J. Butcher, *Inorg. Chim. Acta*, 2009, **362**, 3208.
19 D. D. Perrin, W. L. F. Armarego and D. R. Perrin, *Purification of Laboratory Chemicals*, Pergamon, Oxford, 2nd edn, 1980.
20 N. Ghavale, P. P. Phadnis, A. Wadawale and V. K. Jain, *Indian J. Chem., Sect. A: Inorg., Bio-inorg., Phys., Theor. Anal. Chem.*, 2011, **50**, 22.
21 SIR92 -A. Altomare, G. Cascarano, C. Giacovazzo, A. Guagliardi, M. C. Burla, G. Polidori and M. Camalli, *J. Appl. Crystallogr.*, 1994, **27**, 435.
22 SHELX-G. M. Sheldrick, *Acta Crystallogr., Sect. A: Found. Crystallogr.*, 2008, **64**, 112–122.
23 Crystal structure 3.7.0: Crystal structure Analysis Package, Rigaku, Rigaku/MSC 2000–2005, 9009 New Trials Dr., The Wood, TX 77381, USA.
24 D. J. Watkins, C. K. Prout, J. R. Carruthers and P. W. Betteridge, *CAMERON – A Molecular Graphics Package*, Chemical Laboratory, Oxford (U.K.), 1996.
25 C. K. Johnson, ORTEP-II, Report ORNL-5136, Oak Ridge National Laboratory, Oak Ridge TN, 1976.
26 (*a*) C. Lee, W. Yang and R. G. Parr, *Phys. Rev. B*, 1988, **37**, 785; (*b*) A. D. J. Beck, *Phys. Chem.*, 1993, **98**, 5648; (*c*) A. P. Scott and L. Radom, *J. Phys. Chem.*, 1996, **100**, 16502.
27 M. J. Frisch, G. W. Trucks, H. B. Schlegel, G. E. Scuseria, M. A. Robb, J. R. Cheeseman, G. Scalmani, V. Barone, B. Mennucci, G. A. Petersson, H. Nakatsuji, M. Caricato, X. Li, H. P. Hratchian, A. F. Izmaylov, J. Bloino, G. Zheng, J. L. Sonnenberg, M. Hada, M. Ehara, K. Toyota, R. Fukuda, J. Hasegawa, M. Ishida, T. Nakajima, Y. Honda, O. Kitao, H. Nakai, T. Vreven, J. A. Montgomery Jr., J. E. Peralta, F. Ogliaro, M. Bearpark, J. J. Heyd, E. Brothers, K. N. Kudin, V. N. Staroverov, R. Kobayashi, J. Normand, K. Raghavachari, A. Rendell, J. C. Burant, S. S. Iyengar, J. Tomasi, M. Cossi, N. Rega, N. J. Millam, M. Klene, J. E. Knox, J. B. Cross, V. Bakken, C. Adamo, J. Jaramillo, R. Gomperts, R. E. Stratmann, O. Yazyev, A. J. Austin, R. Cammi, C. Pomelli, J. W. Ochterski, R. L. Martin, K. Morokuma, V. G. Zakrzewski, G. A. Voth, P. Salvador, J. J. Dannenberg, S. Dapprich, A. D. Daniels, Ö. Farkas, J. B. Foresman, J. V. Ortiz, J. Cioslowski and D. J. Fox, GAUSSIAN 09 (Revision A.2), Gaussian, Inc., Wallingford CT, 2009.
28 P. J. Hay and W. R. Wadt, *J. Chem. Phys.*, 1985, **82**, 299.
29 (*a*) C. Gonzalez and H. B. Schlegel, *J. Chem. Phys.*, 1989, **90**, 2154; (*b*) C. Gonzalez and H. B. Schlegel, *J. Phys. Chem.*, 1990, **94**, 5523.
30 A. V. Marenich, C. J. Cramer and D. G. Truhlar, *J. Phys. Chem. B*, 2009, **113**, 6378.
31 The Gibbs free energy value for compounds **1** and **2** was calculated with respect to $PdCl_2$ and $Se(Mes)_2$ by subjecting them to an SMD solvation model ($SMD_{(EtOH)}$) in EtOH whereas compound **3** was calculated with respect to $PdCl_2$, $Se(Mes)_2$ and pyridine-2-thiol in the gas phase.
32 S. Kolay, N. Ghavale, A. Wadawale, D. Das and V. K. Jain, *Phosphorus, Sulfur Silicon Relat. Elem.*, DOI: 10.1080/10426507.2012.757608.

33 A. J. Deeming, M. N. Meah, P. A. Bates and M. B. Hursthouse, *J. Chem. Soc., Dalton Trans.*, 1988, 2193.
34 S. Dey, V. K. Jain, S. Chaudhury, A. Knoedler, F. Lissner and W. Kaim, *J. Chem. Soc., Dalton Trans.*, 2001, 723.
35 S. Dey, V. K. Jain, B. Varghese, T. Schurr, M. Niemeyer, W. Kaim and R. J. Butcher, *Inorg. Chim. Acta*, 2006, **359**, 1449.
36 E. C. Constable, A. M. W. C. Thompson, T. A. Leese, D. G. F. Reese and D. A. Tocher, *Inorg. Chim. Acta*, 1991, **182**, 93.
37 M. Kato, A. Omura, A. Toshikawa, S. Kishi and Y. Sugimoto, *Angew. Chem., Int. Ed.*, 2002, **41**, 3183.
38 J. Ruiz, F. Florenciano, G. Lopez, P. A. Chaloner and P. B. Hitchcock, *Inorg. Chim. Acta*, 1998, **281**, 165.